Article Type: Full Paper

Synthesis and characterization of the hemi-salen ligands and their triboron complexes: Spectroscopy and examination of anticancer properties

Ahmet KILIC[a*], Ismail KOYUNCU[b], Mustafa DURGUN[a], Ismail OZASLAN[a], İbrahim Halil KAYA[a] and Ataman GÖNEL[b]

[a]*Harran University, Department of Chemistry, Art and Science Faculty, 63290, Sanliurfa, Turkey*

[b]*Harran University, Department of Biochemistry, Faculty of Medicine, Sanliurfa 63290, Turkey*

[*] To whom correspondence should be addressed: Harran University, Chemistry Department, TR-63190 Sanlıurfa, Turkey. Tel: +90 414 318 3587, Fax: +90 414 318 3541, e-mail: kilica63@harran.edu.tr; kilica63@hotmail.com

This article has been accepted for publication and undergone full peer review but has not been through the copyediting, typesetting, pagination and proofreading process, which may lead to differences between this version and the Version of Record. Please cite this article as doi: 10.1002/cbdv.201700428

Abstract

The synthesis, spectroscopic properties and *in vitro* cytotoxicity activity of a series of various salen-based triboron complexes have been designed and prepared from hemi-salen **(L_1H_3-L_4H_3)** ligands and $BF_3.Et_2O$ or BPh_3 under simple reaction conditions. The hemi-salen **(L_1H_3-L_4H_3)** ligands and their BF_2 or BPh_2 chelating triboron complexes were characterized by means of NMR (^1H, ^{13}C, ^{19}F and ^{11}B) spectra, FT-IR spectra, UV-Vis spectra, fluorescence spectra, mass spectra, melting point as well as elemental analysis. The triboron **[$L_{(1-4)}(BF_2)_3$]** and **[$L_{(1-4)}(BPh_2)_3$]** complexes were investigated for their absorption and emission properties and these complexes are also good chelates towards boron(III) fragments such as BF_2 or BPh_2 quantum yield in solution reaching up to 38%. The hemi-salen **(L_1H_3-L_4H_3)** ligands and their BF_2 or BPh_2 chelating triboron complexes were tested for the *in vitro* anticancer activity against various the cancer and normal cells (HeLa, DLD-1, ECC-1, PC-3, PNT-1A, and CRL-401O) and it was found that the cell viability of cancer cells was decreased while most of the healthy cells could still be viable. Also, the cytotoxicity studies showed that anti-cancer activity of hemi-salen **(L_1H_3-L_4H_3)** ligands is higher than that of triboron **[$L_{(1-4)}(BF_2)_3$]** and **[$L_{(1-4)}(BPh_2)_3$]** complexes. The hemi-salen **(L_1H_3-L_4H_3)** ligands showing the strongest cytotoxic effect in **PC-3** cells were found to exhibit anticancer activity with apoptosis by increasing the level of ROS in the **PC-3** cells.

Keywords: Hemi-salen ligands, boron complexes, *in vitro* cytotoxicity, reactive oxygen species (ROS), anticancer activity

1. Introduction

The coordination chemistry of tetradentate organic salen and salan-type ligands is well-known as well as the synthesized in one or two steps, inexpensive, air-stable, different structures, structural diversity and rich photophysical properties [1]. One of the main targets in the design of

salen/salan ligands aims at the achievement of tunable electronic, spectroscopic properties and *in vitro* cytotoxicity activity through simple synthetic approaches. Also, solubility and electron-withdrawing/electron-donor characteristics of the compounds can also be regulated as needed. Recently, the tetradentate salen/salan ligand and two fluorine or phenyl atoms chelated tetra-coordinate organoboron complexes have been significantly developed and have undergone widespread application in the fields of materials, molecular machines, OLEDs, probes solar energy collectors, organic electronics and photonics, bioimaging, photodynamic therapy and digital design [2-5] *etc*, is performed by chemists, physicists, engineers and material scientist. For these applications, tetra-coordinate organoboron complexes have received considerable attention due to the generally more stable than other organometallic derivatives in the presence of a weak coordinative B→N and a strong covalent B-O bond [6]. Among four-coordinated boron species, the most widely studied π-conjugated molecular materials are boron difluoride (BF_2) or boron diphenyl (BPh_2) complexes of *N, N*-, *O, O*-, *N, C* and *N, O*-chelating [7] ligands have been selected as ideal candidates to fabricate various application in the fields of textiles, medicinal chemistry, pharmaceutical studies, agriculture, and industry science [8].

By these application fields in mind, the boron compounds containing anticancer studies, which is called as Boron Neutron Capture Therapy (BNCT) [9, 10], have received attention due to the increase in the number of cancer patients in the world. In this context, the development of the effective and stable new boron compounds for anti-cancer agents is one of the main targets for the scientist. Jonnalagadda and coworkers prepared a series of novel functionalized aminobenzoboroxoles as potential anti-cancer agents [11]. Jimenez-Perez et al. synthesized a series of fluorescent molecular rotors of organoboron compounds from Schiff bases and studied their viscosity, reversible thermochromism, cytotoxicity, and bioimaging cells [12]. Akkaya and coworkers prepared a new dimeric BODIPY dye with reduced symmetry, which is ineffective as a photosensitizer unless it is activated by a reaction with intracellular glutathione as differential enhancement of photocytotoxicity targeting of cancer cells [13]. Singh and coworkers developed a

series of *meso*-substituted thienyl BODIPY analogs that are efficient fluorescent probes for cellular bio-imaging and anticancer activity [14]. Hillard et al. used ten new of ferrocenyl chalcone difluoride borate compounds as potential cancer and endothelial cells. This study showed that the ferrocenyl chalcone difluoridoborates furthermore exhibited low cytotoxicity against cancer cells and low morphological activity against epithelial cells [15].

As a contribution to these work, we report the synthesis, spectroscopic and *in vitro* cytotoxic activity of various hemi-salen based triboron **[$L_{(1-4)}(BF_2)_3$]** and **[$L_{(1-4)}(BPh_2)_3$]** complexes have been prepared from hemi-salen **(L_1H_3-L_4H_3)** ligands and $BF_3.Et_2O$ or BPh_3 under simple reaction conditions. These compounds have been characterized by means of NMR (^1H, ^{13}C, ^{19}F and ^{11}B) spectra, FT-IR spectra, UV-Vis spectra, LC-MS spectra, melting point as well as elemental analysis and evaluated for *in vitro* cytotoxicity.

1. Experimental

2. 1. Chemicals and measurements

Without any additional chemical process, the used chemical solvents and starting compounds in this study were purchased from commercial suppliers and used as received. All FT-IR spectra measurements were listed on a Perkin-Elmer Two UATR-FT spectrophotometer in the range of 4000-400 cm^{-1} at room temperature using the ATR accessory. The results of absorption spectra were obtained using a Perkin-Elmer model Lambda 25 spectrometer in the scan range of 200 to 1100 nm using quartz cuvettes at room temperature and the $CHCl_3$ and DMF have been selected as the solvent. Fluorescence spectra were realized on a Perkin-Elmer model LS55 spectrometer and were studied in $CHCl_3$ as a solvent. The elemental analyses of C, H, and N was detected on a LECO CHNS 932 model and founding values were compared with the theoretical values. ^1H and ^{13}C NMR spectra were acquired at 25 ^oC on a Bruker 300 and 75 Tesla spectrometer in DMSO-d_6 as solvent and TMS as an internal

standard, consecutively. Chemical shifts are reported in parts per million (ppm) and coupling constants (*J* values) are given in Hertz. ^{19}F NMR spectra were recorded at 564.6 Tesla in DMSO-d_6 and ^{11}B NMR spectra were acquired at 192.5 Tesla in DMSO-d_6, respectively. To understand whether the target molecules occur, mass spectra were recorded on a Shimadzu LCMS-8040 Triple Quadrupole Liquid Chromatograph Mass Spectrometer (LC-MS/MS). To determine the melting point of all compounds, electrothermal 9100 melting point apparatus was used and obtained values are uncorrected. The fluorescence quantum yields (Φ_s) in $CHCl_3$ as a solvent were estimated from the emission and absorption spectra by a comparative method at the excitation wavelength of 500 nm using Rhodamine B (Φ_r = 0.70) as a reference in C_2H_5OH at room temperature [16]. The fluorescence quantum yields (Φ) were calculated from the following equation:

$$\Phi_s = \Phi_r \times \frac{F_s}{F_r} \times \frac{A_r}{A_s} \times \frac{n_s^2}{n_r^2}$$

Where the subscripts *s* and *r* denote sample and reference respectively, Φ is the fluorescence quantum yield, *A* is the absorbance at the excitation wavelength, *F* is the integrated emission spectrum, and *n* is the refractive index of the solvent at the room temperature [17].

2. 2. In vitro cytotoxic activity

2.2.1. Cell cultures

HeLa (Human Cervical Carcinoma), DLD-1 (Human Colon adenocarcinoma), ECC-1 (Human Cervical Carcinoma), PC-3 (Human Prostate Carcinoma), PNT-1A (Human normal prostate cell), CRL-401O (normal mammary cell) cell line was incubated in Dulbecco's modified Eagle's medium (DMEM) and RPMI-1640 (Sigma Aldrich), supplemented with 10% fetal bovine serum (FBS-Sigma Aldrich), 10 IU/ml penicillin/streptomycin (Sigma Aldrich), and 2m ML-glutamine (Sigma Aldrich) at

37 °C with 5% CO_2 in a 25-ml flask. The cells were used for the assays performed in this study when reached to 80-90% confluence.

2.2.2. Cell viability assay (MTT)

The MTT assay was performed to analyze the proliferation of normal and cancer cells. Cells (5×10^4/ml) were seeded in 96 well plates and maintained for 24 h under standard conditions (37 °C, and 5% of CO_2). The synthesized compounds treated three times in different concentrations between ranges of 0-200 µM on wells of cells grown. After 48 h of incubation, the medium was removed and then MTT assay was performed. After incubation for 4 h, the supernatant was removed and the obtained formazan crystals were dissolved in 100 µl of DMSO (Sigma). The mixture was stirred for 10 min on a microtiter plate shaker and optical density (at 570 nm) was measured using microplate reader (Multiskan GO, Thermo Fisher Scientific, Waltham, MA), and the viability rate was calculated.

Cell viability was expressed as the percentage of untreated cells that served as the control group and was designated as 100%. Cytotoxicity was expressed as mean percentage increase relative to the unexposed control ± standard deviation. Control values were set at 0% cytotoxicity. Cytotoxicity data (where appropriate) was fitted to a sigmoidal curve and a four-parameter logistic model was used to calculate the IC_{50}, which is the concentration of material causing 50% inhibition in comparison to the untreated controls. The mean IC_{50} is the concentration of material that reduces cell growth by 50% under the experimental conditions and is the average of at least three independent measurements that were reproducible and statistically significant. The IC_{50} values were reported at ±95% confidence intervals (±95% CI). This analysis was performed with Graph Pad Prism (San Diego, CA, USA).

2.2.3. Apoptosis detection by Annexin V-FITC and propidium iodide staining

The synthesized hemi-salen ligands **(L_1H_3-L_4H_3)** and their triboron complexes **[$L_{(1-4)}(BF_2)_3$]** and **[$L_{(1-4)}(BPh_2)_3$]** were treated three times with different concentrations between 2.5-10-25 µM on wells after new media were added to the wells. Cells (1×10^6 cells) were harvested after 48 hours. For apoptotic analysis, the cells were stained using FITC Annexin V Apoptosis Detection Kit I (BD Biosciences, New Jersey, USA) was used according to the manufacturer's recommendations. Briefly, Harvested cells were centrifuged at 1200 rpm for 5 min and suspended in 1X Binding buffer. 5 µL fluorochrome-conjugated Annexin V and 5 µL Propidium Iodide Staining or 7-Amino-Actinomycin D (7AAD) were added and incubated at room temperature for 15 min in the dark. Flow cytometry (BD Via, New Jersey, USA) analytic method was used after incubation.

2.2.4. Determination of intracellular ROS generation with DCFH-DA

Intracellular ROS was measured using the 2',7'-dichlorofluorescein diacetate (DCFH-DA) fluorescent probe. Briefly, cells were pre-treated with hemi-salen **(L_3H_3)** ligand at 2,5- 25 µM concentrations. After 24 h of incubation, the medium was discarded and the cells were washed twice with PBS. The cells were treated with 10 µM DCFH-DA for 30 min in the dark. Then, the cells were washed twice with PBS to remove the extracellular components, and DCFH-DA fluorescence was detected using a spectrofluorometer (SPECTRAmax M5) with excitation and emission wavelengths of 470 and 530 nm, respectively.

2. 3. Synthesis of the hemi-salen ligands (L_1H_3-L_4H_3)

The hemi-salen ligands **(L_1H_3)** and **(L_3H_3)** were synthesized following the procedure with some modifications [18, 19]. The ligands **(L_1H_3-L_4H_3)** were synthesized by reacting the corresponding 3,5-Di-*tert*-butyl salicylaldehyde (2.10 g, 9.0 mmol) for ligand **(L_1H_3)**, 5-methoxy salicylaldehyde (1.37 g, 9.0 mmol) for ligand **(L_2H_3)**, 3,5-Dibromosalicylaldehyde (2.52 g, 9.0 mmol) for ligand **(L_3H_3)**, and 2-Hydroxynaphthaldehyde (1.55 g, 9.0 mmol) for ligand **(L_4H_4)** with tris-(2-aminoethyl) amine (0.44 g, 3.0 mmol) in 60 mL of EtOH at room

temperature and in the presence of 1-2 drop formic acid as catalyst. Then, the yellow reaction mixtures were stirred for 6 hours at reflux temperature for the formation of three branches ligands. Later, the mixtures were cooled to room temperature and the half of solvent was evaporated and the solution was placed in the laboratory for overnight. The obtained yellow crystals were washed three times with diethyl ether and n-hexane. Recrystallization from $CHCl_3/CH_3OH$ by slow evaporation afforded pure hemi-salen ligands **(L_1H_3-L_4H_3)** obtained. Analytical results are given as supplementary information for all hemi-salen ligands **(L_1H_3-L_4H_3)**.

2. 4. Synthesis of the fluorine triboron complexes

To a 50 mL round-bottomed flask containing 20 mL benzene and 5 mL toluene were added ligand **(L_1H_3)** (0.6 mmol, 0.48 g), ligand **(L_2H_3)** (0.6 mmol, 0.33 g), ligand **(L_3H_3)** (0.6 mmol, 0.55 g), or ligand **(L_4H_3)** (0.6 mmol, 0.37 g) under N_2 atmosphere. After addition of $BF_3.OEt_2$ (5.40 mmol, ~0.7 mL) to the reaction mixture, stirring was continued for 30 min. with the solution turning from yellow to light red. Then, 0.5 mL triethylamine (Et_3N) was added to the reaction flask and the mixtures were refluxed for 4 hours. The desired products were collected by filtration as a light-red or red. The light-red or red products were washed diethyl ether and hexane, followed by the products dried in air. Recrystallization from $CHCl_3$/MeOH (1:3) by slow evaporation afforded pure compounds. Analytical results are given as supplementary information for all fluorine triboron complexes.

2. 5. Synthesis of the phenyl triboron complexes

In a typical experiment, to a 50 mL round-bottomed flask containing 25 toluene and 5 mL THF were added ligand **(L_1H_3)** (0.6 mmol, 0.48 g), ligand **(L_2H_3)** (0.6 mmol, 0.33 g), ligand **(L_3H_3)** (0.6 mmol, 0.55 g), or ligand **(L_4H_3)** (0.6 mmol, 0.37 g) under N_2 atmosphere and stirring had continued for 40 min. After addition of triphenyl boron (BPh_3) (2.7 mmol, 065 g) was added to the reaction flask, the color of the mixtures turning from yellow to light-green.

The reaction mixtures were stirred at room temperature for 8 hours and were refluxed for 4 hours until reaction completion, as judged by TLC. The completed reactions were cooled to room temperature and all the volatiles were evaporated under vacuum. The desired crystalline products were collected by filtration as a light-green. The pure microcrystalline phenyl triboron complexes were washed with Et_2O and n-hexane and kept at 25 ^oC to afford the corresponding phenyl triboron complexes. Analytical results are given as supplementary information for all phenyl triboron complexes.

3. Results and discussion

3. 1. Synthesis and characterization

The hemi-salen ligands **(L_1H_3-L_4H_3)** have been synthesized via the condensation reaction of a 3,5-di-*tert*-butyl salicylaldehyde for ligand **(L_1H_3)** [18], 5-methoxy salicylaldehyde for ligand **(L_2H_3)**, 3,5-dibromo salicylaldehyde for ligand **(L_3H_3)** [19], and 2-hydroxy-1-naphthaldehyde for ligand **(L_4H_4)** with tris-(2-aminoethyl) amine in EtOH under reflux conditions and in the presence of 1-2 drop formic acid as catalyst (Scheme 1), and also their characterization data was presented in the supporting information part. Then, the reaction of the hemi-salen ligands **(L_1H_3-L_4H_3)** with $Et_2O.BF_3$ was carried out under an N_2 atmosphere in the mixture of benzene and toluene using Et_3N as a base to afford fluorine triboron complexes **[$L_{1\text{-}4}(BF_2)_3$]** in good yield up to 68% (Scheme 2). Finally, the phenyl triboron complexes **[$L_{1\text{-}4}(BPh_2)_3$]** have been synthesized by using the hemi-salen ligands **(L_1H_3-L_4H_3)** with BPh_3 under an N_2 atmosphere in the mixture of toluene and THF in good yield up to 66% (Scheme 2). The structure of the hemi-salen ligands and their fluorine with phenyl triboron complexes were unambiguously characterized by NMR (^1H, ^{13}C, ^{19}F and ^{11}B) spectra, FT-IR spectra, UV-Vis spectra, LC-MS spectra (Figure S14-S15), Fluorescence spectra, melting point as well as elemental analysis. The found and the calculated percentages of all compounds were confirmed by C, H, N analysis and results agree with each other and these prove the proposed molecular formulas. We have attempted to prepare single crystals of the hemi-salen ligands and their fluorine with

phenyl triboron complexes in various solvents, but unfortunately, we could not obtain single any crystals suitable for X-ray diffraction studies for all compounds.

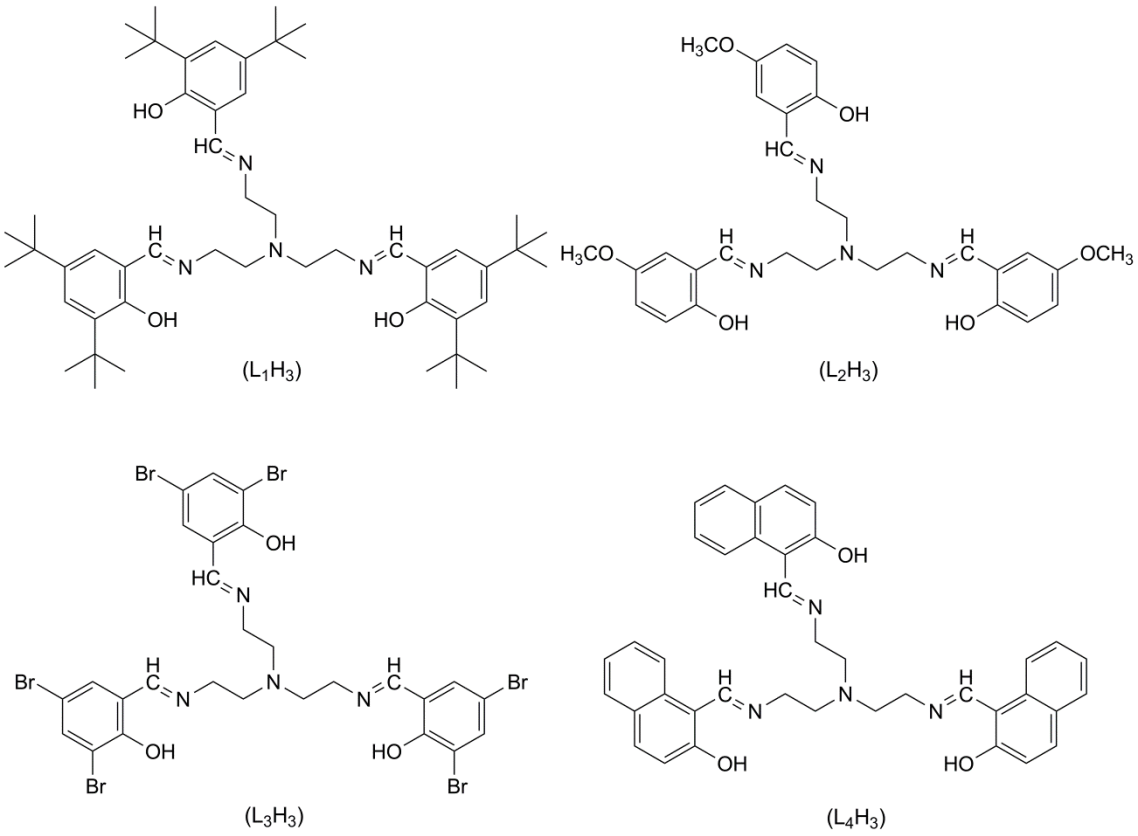

Scheme 1. The selected hemi-salen ligands **($L_{1\text{-}4}H_3$)** for this study

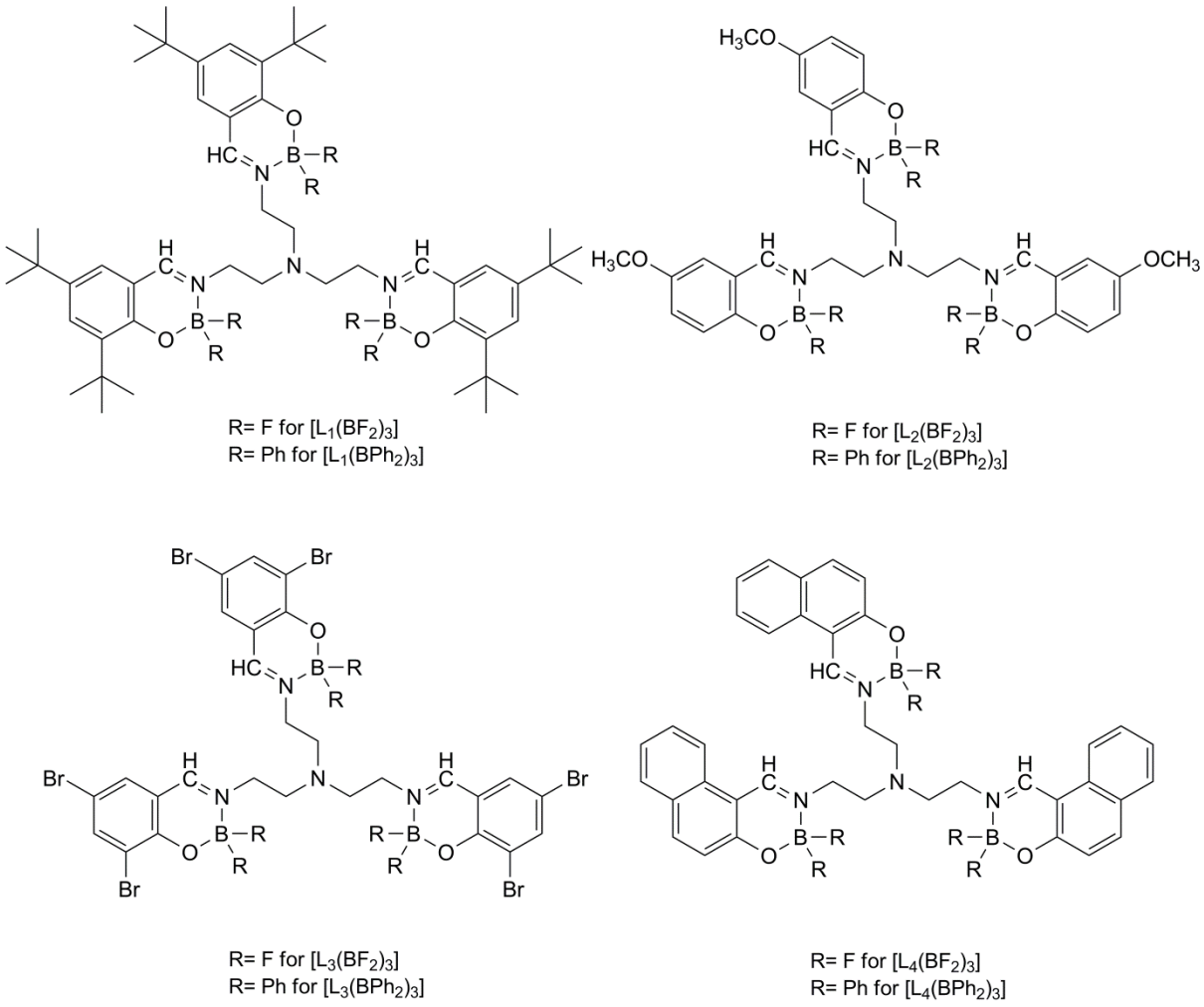

Scheme 2. The structure of the proposed the fluorine triboron complexes **[$L_{1\text{-}4}(BF_2)_3$]** and phenyl triboron complexes **[$L_{1\text{-}4}(BPh_2)_3$]**

3. 2. Spectroscopic properties

To have information about all compounds, The FT-IR spectra of ligands **(L_1H_3-L_4H_3)** and their fluorine **[$L_{1\text{-}4}(BF_2)_3$]** with phenyl **[$L_{1\text{-}4}(BPh_2)_3$]** triboron complexes were compared. The FT-IR stretching vibration data of all compounds are given in the supporting information part and Figure S1-S4. In the FT-IR spectra of the hemi-salen ligands **(L_1H_3-L_4H_3)**, the most obvious difference was the appearance for intermolecular H-bond υ(OH···N=CH) at range 3564-2364 cm^{-1} and the (C=N) imine at range 1633-1620 cm^{-1} [20], whereas the intermolecular H-bond υ(OH···N=CH) was disappeared and the (C=N)

imine stretching frequencies shifts to different wavenumbers (1647-1613 cm^{-1}) in the FT-IR spectra of fluorine and phenyl triboron complexes, as expected (Figure S1-S4) [21]. These results show that the deprotonation of the phenolic proton prior to coordination and confirm the formation of the fluorine triboron **$[L_{1\text{-}4}(BF_2)_3]$** and phenyl triboron **$[L_{1\text{-}4}(BPh_2)_3]$** complexes. However, the FT-IR spectra of the different hemi-salen ligands **$(L_1H_3\text{-}L_4H_3)$** compare with the fluorine triboron **$[L_{1\text{-}4}(BF_2)_3]$** and phenyl triboron **$[L_{1\text{-}4}(BPh_2)_3]$** complexes, the free phenolic protons are disappearance of the *ortho* υ(O-H) peaks of the ligands **$(L_1H_3\text{-}L_4H_3)$** and a new stretching frequency were observed at range 1297-1290 cm^{-1} for B-O, at range 1057-1054 cm^{-1} for B-N, at range 524-519 cm^{-1} for B-F of the fluorine triboron **$[L_{1\text{-}4}(BF_2)_3]$** complexes and at range 1186-1186 cm^{-1} for B-O, at ~1026 cm^{-1} for B-N, at ~ 883 cm^{-1} for B-Ph of phenyl triboron **$[L_{1\text{-}4}(BPh_2)_3]$** complexes, respectively, which the most powerful evidence that the BF_2 or BPh_2 groups was successfully connected into the four coordinate triboron complexes [22]. Furthermore, the other stretching frequencies in the FT-IR spectra of all compounds are given in the supporting information part also confirm the formation of the proposed compounds.

Further evidence for the formation of the salen ligands **$(L_1H_3\text{-}L_4H_3)$** and their triboron **$[L_{1\text{-}4}(BF_2)_3]$** and **$[L_{1\text{-}4}(BPh_2)_3]$** complexes were obtained from the ^{1}H NMR, ^{13}C NMR, ^{19}F NMR, and ^{11}B NMR spectra (see supporting information and Figure S5-S11). The ^{1}H NMR signals belonging to the OH protons are readily distinguishable and the disappearance of the downfield H-bonded OH protons (δ ≈ 13-15 ppm) of the salen-type **$(L_1H_3\text{-}L_4H_3)$** gives the first indication for the formation of triboron complexes [1, 23] and also the disappearance of the readily distinguishable OH protons confirm the binding of the boron atoms to the oxygen. The proton peaks of the azomethine groups in fluorine triboron complexes **$[L_{1\text{-}4}(BF_2)_3]$** (at range δ = 8.92-8.53 ppm) and phenyl triboron complexes **$[L_{1\text{-}4}(BPh_2)_3]$** (at range δ = 9.06-8.04 ppm) are significantly shifted to the low or high field in comparison with those of the formed hemi-salen ligands **$(L_1H_3\text{-}L_4H_3)$** (at range δ = 9.08-8.26 ppm), resulting from the electron deficient/electron excess nature of BF_2 or BPh_2 moiety. Moreover, the NMR data show that the chemical shift of ^{13}C NMR peaks supports the formation of the different

hemi-salen ligands **(L_1H_3-L_4H_3)** and their fluorine **[$L_{1\text{-}4}(BF_2)_3$]** with phenyl **[$L_{1\text{-}4}(BPh_2)_3$]** triboron complexes in DMSO-d_6 gave signals in good agreement with the proposed structures. In the ^{13}C NMR spectra of ligands **(L_1H_3-L_4H_3)** and their fluorine **[$L_{1\text{-}4}(BF_2)_3$]** with phenyl **[$L_{1\text{-}4}(BPh_2)_3$]** triboron complexes, the chemical shifts observed at range δ = 177.80-155.82 ppm assigned to imine (H*C*=N) carbons and at range δ = 160.28-103.57 ppm assigned to aromatic (Ar-*C*H) carbons, respectively. These chemical signals from imine (H*C*=N) and aromatic (Ar-*C*H) carbons were in the expected range. In addition, in the aromatic region of ^{13}C NMR spectra for the phenyl **[$L_{1\text{-}4}(BPh_2)_3$]** triboron complexes have seen that there are aromatic carbons of numerous aromatic carbons signals resulting from the nature of BPh_2 moiety, as expected.

In the ^{11}B NMR spectra of the fluorine **[$L_{1\text{-}4}(BF_2)_3$]** with phenyl **[$L_{1\text{-}4}(BPh_2)_3$]** triboron complexes, only one boron signal observed in the range of δ = -0.92 to -0.98 ppm for fluorine triboron **[$L_{1\text{-}4}(BF_2)_3$]** complexes and in the range of δ = 1.09 to 1.16 ppm for phenyl triboron **[$L_{1\text{-}4}(BPh_2)_3$]** complexes due to the same chemical environment for the three boron atoms of each compound (Figure 1 and 2), which is confirm the formation of four-coordinate *N, O*-chelated triboron complexes [6, 23] and indicate N→B bonds to be predominant in DMSO-d_6 solution. However, the fluorine **[$L_{1\text{-}4}(BF_2)_3$]** with phenyl **[$L_{1\text{-}4}(BPh_2)_3$]** triboron complexes showed different chemical resonances in ^{11}B NMR spectra, suggesting the alteration of electronic properties because of the presence of the various electron withdrawing/donor groups on the aromatic ring in triboron complexes (Figure 1). Furthermore, the fluorine triboron **[$L_{1\text{-}4}(BF_2)_3$]** complexes were also characterized by ^{19}F NMR spectroscopy. The ^{19}F NMR resonance of these triboron complexes is in the range of δ = -145.62 to -146.32 ppm, confirming the formation of four-coordinate triboron complexes. The absence of quartets in the ^{19}F NMR spectra reveals that there may be a fast relaxation of the quadrupolar boron nuclei at room temperature (Figure 2) [23, 24].

3. 3. Photophysical properties

The UV/Vis absorption and emission spectral data of all hemi-salen ligands and their triboron complexes are given in the supporting information part and Table 1. As examples, the normalized absorption spectra of the hemi-salen ligands **(L_1H_3-L_4H_3)** and their fluorine **[$L_{1\text{-}4}(BF_2)_3$]** with phenyl **[$L_{1\text{-}4}(BPh_2)_3$]** triboron complexes at range 2.10^{-5}-2.10^{-7} mol L^{-1} and in $CHCl_3$ or DMF are shown in Figure 3 and S12-S13. Formation of the fluorine **[$L_{1\text{-}4}(BF_2)_3$]** with phenyl **[$L_{1\text{-}4}(BPh_2)_3$]** complexes from the hemi-salen ligands causes a moderately red or blue shift of the absorption bands. It was clear that salen ligands **(L_1H_3-L_4H_3)** exhibited similar features and obvious absorption bands at range 241-446 nm in $CHCl_3$ and at range 233-431 nm in DMF, respectively. The fluorine **[$L_{1\text{-}4}(BF_2)_3$]** with phenyl **[$L_{1\text{-}4}(BPh_2)_3$]** triboron complexes containing the center amine group and different aromatic rings of ligands have relatively intense absorption bands centered at range 253-589 nm in $CHCl_3$ and at range 250-447 nm in DMF, respectively, which are assigned to the generally $\pi\rightarrow\pi^*$ or $n\rightarrow\pi^*$ transition involving molecular orbitals essentially localized on the azomethine (C=N) group with the aromatic ring and the intramolecular charge transfer (ICT) transition [1, 25-30]. Moreover, the red or blue shifts in $CHCl_3$ or DMF solvents of the absorption bands of the fluorine **[$L_{1\text{-}4}(BF_2)_3$]** with phenyl **[$L_{1\text{-}4}(BPh_2)_3$]** triboron complexes compared with those of salen ligands **(L_1H_3-L_4H_3)** resulted from different electron-withdrawing/donor abilities on the aromatic ring and maybe the difluoro or diphenyl boron units. Apart from the mentioned band shift, the results of the absorption spectra are very similar to the hemi-salen ligands and their fluorine **[$L_{1\text{-}4}(BF_2)_3$]** with phenyl **[$L_{1\text{-}4}(BPh_2)_3$]** triboron complexes which reveal that the absorption bands usually are salen ligand-centered.

The obtained of the emission spectra of fluorine **[$L_{1\text{-}4}(BF_2)_3$]** and phenyl **[$L_{1\text{-}4}(BPh_2)_3$]** triboron complexes in $CHCl_3$ are given in Figure 4-5 and Table 1. As far as the fluorescence spectra are concerned, the emission spectra of each kind of triboron complexes were located at between 515-438 nm when excited at range 382-350 nm for fluorine **[$L_{1\text{-}4}(BF_2)_3$]** triboron complexes and at

between 528-492 nm when excited at range 424-405 nm for phenyl **[$L_{1\text{-}4}(BPh_2)_3$]** triboron complexes, respectively. In addition to the observed fluorescence spectra results, all triboron complexes showed red shifted and more complicated since the electron-withdrawing/donating or non-substituted groups on the aromatic rings are only one of the influencing factors for fluorine or phenyl triboron complexes. The emission spectra of the **[$L_4(BF_2)_3$]** and **[$L_4(BPh_2)_3$]** triboron complexes in $CHCl_3$, the three naphthyl groups on the ligands, are a little red-shifted and small Stokes shifts in comparison with other triboron complexes (see Table 1). This is possibly occurring due to the replacement of three naphthyl groups with the electron-withdrawing/donating groups on the aromatic rings, which the transition to different electronically excited states or the increased emission intensity due to charge transfer nature and the extension of the linear π-conjugation. All other fluorine **[$L_{1\text{-}4}(BF_2)_3$]** and phenyl **[$L_{1\text{-}4}(BPh_2)_3$]** triboron complexes have large red-shifted and large Stokes shifts in the range of 457-528 nm and 135-104 nm, respectively. Among them, the complexes **[$L_2(BF_2)_3$]** and **[$L_2(BPh_2)_3$]** have the large red-shifted peaks and large Stokes shifts value due to the presence of the electron donor methoxy groups on the salen ligand **(L_2H_3)** [31] and also are supposed to be ascribed to the remarkable structural relaxation from the excited state to the ground state as the result of free rotation of the three branch-salen ligands, which inspired us for the further applications of tetra-coordinate boron chemistry.

Table 1. The fluorescence spectrum data and quantum yields of triboron complexes in $CHCl_3$

Compound	UV/Vis λ_{max} (nm)	λ_{ex} (nm)	λ_{em} (nm)	Stokes shift (nm)	Φ_s
$[L_1(BF_2)_3]$	350	350	485	135	0.17
$[L_2(BF_2)_3]$	386	380	515	135	0.23
$[L_3(BF_2)_3]$	353	353	457	104	0.22
$[L_4(BF_2)_3]$	372	382	438	56	0.26
$[L_1(BPh_2)_3]$	402	405	510	105	0.38
$[L_2(BPh_2)_3]$	424	424	528	104	0.19
$[L_3(BPh_2)_3]$	406	406	510	104	0.10
$[L_4(BPh_2)_3]$	412	412	492	80	0.19

3. 4. *In vitro* cytotoxic activity

In this study, after synthesizing and characterizing the hemi-salen ligands **(L_1H_3-L_4H_3)** and their fluorine **$[L_{1\text{-}4}(BF_2)_3]$** with phenyl **$[L_{1\text{-}4}(BPh_2)_3]$** triboron complexes, these compounds were tested for their general cytotoxicity against various the cancer cells (HeLa, DLD-1, ECC-1, PC-3) and normal cells (PNT-1A, and CRL-401O) by using the MTT assay technique. For the positive control, the compound 5-Fu (5-fluorouracil) used as reference chemotherapeutic agent in this study. The IC_{50} results (concentration required to inhibit tumor cell proliferation by 50%) of the synthesized hemi-salen ligands and their triboron complexes are given in Table 2. These cytotoxicity results showed that the cancer of cell viability was decreased while most of the healthy cells could still be viable. Also, cytotoxicity results showed that anticancer activity of hemi-salen **(L_1H_3-L_4H_3)** (IC_{50}: 5.68-92.91 μM) ligands are higher compared to the their triboron **$[L_{(1\text{-}4)}(BF_2)_3]$** and **$[L_{(1\text{-}4)}(BPh_2)_3]$** complexes.

However, the hemi-salen **(L_3H_3)** ligand shows higher cytotoxic activity on the **PC-3** cancer cell compared to the other hemi-salen ligands of this study in different concentrations between ranges of 0-200 µM on wells of cells grown for 24 h. As DMSO was the solvent used for the compounds (Table 2). The cytotoxic effects of the hemi-salen **(L_3H_3)** ligand for **PC-3** and **PNT-1A** cells were determined to be IC_{50}: 5.68-20.33 µM and the cytotoxic effects of the normal prostate cell (PNT-1A) were very low compared to the cancer cells **(PC-3)**. Thus, the molecular mechanism of the hemi-salen **(L_3H_3)** ligand, which exhibits the strongest cytotoxic effect from 12 molecules synthesized, on the cancer cell **(PC-3)** has been investigated. The effect of the hemi-salen **(L_3H_3)** ligand on cell growth of human prostate cancer **PC-3** cells is given in Figure 6. **PC-3** cells were treated with different concentrations of the hemi-salen **(L_3H_3)** ligand (0- 200 µM) or vehicle for 48 hours, respectively. It was found that the hemi-salen **(L_3H_3)** ligand was active against prostate cancer **PC-3** cells, and the growth inhibition and killing of **PC-3** cells by the hemi-salen **(L_3H_3)** ligand were attributed to the induction of apoptosis as demonstrated by an increase in annexin V and PI binding.

Table 2. Cytotoxicity activity of **($L_{1\text{-}4}H_3$)**, **[$L_{1\text{-}4}(BF_2)_3$]** and **[$L_{1\text{-}4}(BPh_2)_3$]** on tumor cell lines and normal cell lines.

Compound	**IC_{50} (μM)[a,b]**					
	Cancer Cell				**Normal Cell**	
	DLD-1	**PC3**	**HeLa**	**ECC-1**	**CRL-4010**	**PNT-1A**
(L_1H_3)	80.53	13.46	100.03	>500	185.00	123.20
(L_2H_3)	33.06	15.72	25.10	92.91	35.69	43.22

(L_3H_3)	16.69	5.68	13.25	20.67	14.04	20.33
(L_4H_3)	15.27	12.76	10.38	13.31	14.89	34.44
[$L_1(BF_2)_3$]	76.70	27.57	52.98	149.58	109,72	78.65
[$L_2(BF_2)_3$]	152.20	53.09	130.04	209.88	159.97	278.60
[$L_3(BF_2)_3$]	413.44	160.20	>500	155,48	102.30	230.40
[$L_4(BF_2)_3$]	39.29	13.83	>500	8.29	8.14	55.40
[$L_1(BPh_2)_3$]	375.82	>500	>500	189.47	>500	430.30
[$L_2(BPh_2)_3$]	266.74	399.81	386.44	498.75	290.16	345.50
[$L_3(BPh_2)_3$]	253.50	>500	>500	>500	113.11	233.30
[$L_4(BPh_2)_3$]	>500	>500	>500	>500	>500	>500
5-Fu	50.90	45.20	19.20	30.20	23.33	21.44

[a] Values are means of three independent experiments.

[b] IC_{50} values determined at 48 h.

Recent papers have demonstrated that reactive oxygen species (ROS) plays a key role in anticancer activities of various compounds [14]. Therefore, we investigated the role of ROS in the hemi-salen **(L_3H_3)** ligand-induced apoptosis in prostate cancer **PC-3** cells by using 2',7'-dichlorofluorescein diacetate (DCFH-DA) fluorescent probe. ROS is intracellularly generated as by products of normal aerobic metabolism or as second messengers in various signal transduction pathways or in response to environmental stress [32, 33]. The generation of ROS is part of the

mechanism by which most chemotherapeutic agents kill tumor cells [34-36]. Our present findings demonstrated for the hemi-salen **(L_3H_3)** ligand. In the hemi-salen **(L_3H_3)** ligand-induces ROS generation in **PC-3** cells. Generation of ROS plays an important role in proapoptotic activities of various anticancer agents. Therefore, we investigated whether generation of intracellular ROS is part of the mechanism by which in the hemi-salen **(L_3H_3)** ligand induces apoptosis in **PC-3** cells. As shown in Figure 7, after exposure to the different concentration of the hemi-salen **(L_3H_3)** ligand for 24 hours, the DCF fluorescence intensity was found to be increased compared with vehicle-treated control. The obtained results are consistent with the results of previous studies showing the participation of ROS in the killing of astrocytoma CRT-MG and breast cancer MCF-7 cells [37, 38]. The role of ROS in the hemi-salen **(L_3H_3)** ligand-induced apoptosis in **PC-3** cells was further confirmed by annexin V-assay implying that ROS may have a role in the activation of apoptotic process induced by the hemi-salen **(L_3H_3)** ligand in the **PC-3** cell.

As shown in Figure 8, the effect of the hemi-salen **(L_3H_3)** ligand on apoptosis of human prostate cancer **PC-3** cells. Apoptosis of **PC-3** cells incubated with different concentrations of the hemi-salen **(L_3H_3)** ligand (0, 2.5, 5.0, 10.0, 25.0 μM) and vehicle (served as a control) for 48 hours was examined using flow cytometry with annexin V-FITC apoptosis detection kit. Annexin V-FITC binding while remaining propidium iodide (PI) negative can indicate phosphatidylserine (PS) exposure on the outer leaflet of the plasma membrane without membrane damage, which is the feature of an early stage of apoptosis. Pictures are representative of three independent experiments. Percentage of analysis of annexin V/PI flow cytometry of PC-3 cells treated with the hemi-salen **(L_3H_3)** ligand. At least 10.000 cells were analyzed from per sample, and quadrant analysis was performed.

4. Conclusion

We have reported four hemi-salen ligands and theirs BF_2 or BPh_2 chelating triboron complexes have been shown to exhibit good spectroscopic and fluorescence properties that quantum yield in $CHCl_3$ reaching up to 38%. These complexes have been shown too easy to synthesize and modulate, environmental friendly, cost effective and stable to air. The emission spectra of the **$[L_4(BF_2)_3]$** and **$[L_4(BPh_2)_3]$** triboron complexes are a little red-shifted and small Stokes shifts in a comparison with other triboron complexes in $CHCl_3$ because of the introduction of the three naphthyl groups on the ligands. The present study evaluated the effects of the hemi-salen ligands and their triboron compounds on cytotoxic effect on cancer cells (HeLa, DLD-1, ECC-1, PC-3) and normal cells (PNT-1A, and CRL-401O) and apoptotic and intracellular reactive oxygen species (ROS) generation activity in **PC-3** cells. **PC-3** cells were treated with the hemi-salen **(L_3H_3)** ligand at different concentrations. Intracellular ROS generation was measured using the 2',7'-dichlorofluorescein diacetate fluorescent probe. Especially, the hemi-salen **(L_3H_3)** ligand has shown low cytotoxicity, which is good for new potential chemotherapeutic agents for treating malignant cancers in near future.

Acknowledgement

This work was supported by the Research Fund of Harran University (*HUBAK Projects No: 16047)* Sanliurfa, Turkey

References

[1] J. Cheng, K. Wei, X. Ma, X. Zhou, and H. Xiang, J. Phys. Chem. C 117 (2013) 16552-16563.

[2] X. Li, G. Ji, Y.-A. Son, Dyes and Pigments 124 (2016) 232-240.

[3] S. Guieu, F. Cardona, J. Rocha and A. M. S. Silva, New J. Chem. 38 (2014) 5411-5414.

[4] S. Erten-Ela, M. D. Yilmaz, B. Icli, Y. Dede, S. Icli and E. U. Akkaya, Org. Lett. 10 (2008) 3299-3302.

[5] T.-I. Kim, J. Park, S. Park, Y. Choi and Y. Kim, Chem. Commun. 47 (2011) 12640-12642.

[6] F. Qiu, F. Zhang, R. Tang, Y. Fu, X. Wang, S. Han, X. Zhuang, and X. Feng, Org. Lett. 18 (2016) 1398-1401.

[7] R. Deng, L. Li, M. Song, S. Zhao, L. Zhou and S. Yao, CrystEngComm, 18 (2016) 4382-4387.

[8] H. Temel, S. Pasa, M. Aydemir, Tetrahedron: Asymmetry 26 (2015) 1058-1064.

[9] J. G. Penland, Environ. Health Perspect. 102 (1994) 65-72.

[10] S. Pasa, S. Aydın, S. Kalaycı, M. Boğa, M. Atlan, M. Bingul, F. Şahin, H. Temel, Journal of Pharmaceutical Analysis 6 (2016) 39-48.

[11] P. Suman, B. P. Patel, A. V. Kasibotla, L. N. Solano, S. C. Jonnalagadda, J. Organomet. Chem. 798 (2015) 125-131.

[12] M. Ibarra-Rodriguez, B. M. Munnoz-Flores, H. V. R. Dias, M. Sanchez, A. Gomez-Trevinno, R. Santillan, N. Farfan, and V. M. Jimenez-Perez, J. Org. Chem. 82 (2017) 2375-2385.

[13] S. Kolemen, M. Isık, G. M. Kim, D. Kim, H. Geng, M. Buyuktemiz, T. Karatas, X. F. Zhang, Y. Dede, J. Yoon, E. U. Akkaya, Angew. Chem. Int. Ed. 54 (2015) 5340-5344.

[14] T. Gayathri, A. K. Barui, S. Prashanthi, C. R. Patra and S. P. Singh, RSC Adv. 4 (2014) 47409-47413.

[15] J. P. Monserrat, R. I. Al-Safi, K. N. Tiwari, L. Quentin, G. G. Chabot, A. Vessieres, G. Jaouen, N. Neamati, E. A. Hillard, Bioorganic & Medicinal Chemistry Letters 21 (2011) 6195-6197.

[16] (a) R. A. Velapoldi, H. H. Tønnesen, J. Fluoresc. 14 (2004), 465; (b) P. Wei and D. A. Atwood, Inorg. Chem. 36 (1997) 4060-4065.

[17] J. R. Albani, Principles and Applications of Fluorescence Spectroscopy, Wiley-Blackwell, (2007) 88-113.

[18] P. Dröse and J. Gottfriedsen, Z. Anorg. Allg. Chem. 634 (2008) 87-90.

[19] W. Marritt, United States Patent, Patent No: US 6,776,830 B2, Date of Patent: Aug. 17, 2004.

[20] B. C.E. Makhubela, M. Meyer, G. S. Smith, J. Organomet. Chem. 772-773 (2014) 229-241.

[21] A. Kilic, F. Alcay, M. Aydemir, M. Durgun, A. Keles, A. Baysal, Spectrochim. Acta Part A 42 (2015) 62-72.

[22] A. Kilic, M. Aydemir, M. Durgun, N. Meric, Y.S. Ocak, A. Keles, H. Temel, J. Fluorine Chem. 162 (2014) 9-16.

[23] K. Dhanunjayarao, V. Mukundam M. Ramesh, and K. Venkatasubbaiah, Eur. J. Inorg. Chem. (2014) 539-545.

[24] N. N. Shapetko, L. N. Kurkovskaya, V. G. Medvedeva, A. P. Skoldinov, L. K. Vasyanina, Zh. Strukt. Khim. 10 (1969) 824-826.

[25] Y. Zhan, Y. Xu, P. Yang, H. Zhang, Y. Li, J. Liu, Tetraheron Lett. 57 (2016) 5385-5389.

[26] J. Sun, J. Sun, W. Mi, P. Xue, J. Zhao, L. Zhai and R. Lu, New J. Chem. 41 (2017) 763-772.

[27] S. C. Wang, G. W. Men, L. Y. Zhao, Q. F. Hou, S. M. Jiang, Sens. Actuators B: Chem. 145 (2010) 826-831.

[28] C. Gou, S. H. Qin, H. Q. Wu, Y. Wang, J. Luo, X. Y. Liu, Inorg. Chem. Commun. 14, (2011) 1622-1625.

[29] S. Di Bella, I. Fragala, I. Ledoux, M. A. Diaz-Garcia,T. J. Marks, J. Am. Chem. Soc. 119 (1997) 9550-9557.

[30] R. C. Felicio, E. T. G. Cavalheiro, E. R. Dockal, Polyhedron 20 (2001) 261-268.

[31] X. Li, G. Ji, Y. A. Son, Dyes and Pigments 124 (2016) 232-240.

[32] H. Nohl, A. V. Kozlov, L. Gille, K. Staniek, Biochem Soc Trans 31 (2003) 1308-1311

[33] S. Raha, B. H. Robinson, Amer. J. Med. Genet. 106 (2001) 62-70.

[34] J. Gao, X. Liu, B. Rigas, Proc. Natl. Acad. Sci. USA 102 (2005) 17207-17212.

[35] B. Ramanathan, K. Y. Jan, C. H. Chen, T. C. Hour, H. J. Yu, Y. S. Pu, Cancer Res. 65 (2005) 8455-8460

[36] Y. Sun, B. Rigas, Cancer Res. 68 (2008) 8269-8277.

[37] A. D. Kim, K. A. Kang, R. Zhang, C. M. Limb, H. S. Kimc, D. H. Kimd, Y. J. Jeona, C. H. Lee, J. Parke, W. Y. Chang, J. W. Hyunb, Environ. Toxicol. Phar. 30 (2010) 134-140.

[38] K. Choi, C. Choi, Cancer Res. Treat. 41 (2009) 36-44.

CAPTION

Figure 1. The ^{11}B-NMR spectra of $[L_1(BF_2)_3]$ complex in DMSO

Figure 2. The ^{19}F-NMR spectra of $[L_1(BF_2)_3]$ complex in DMSO

Figure 3. The UV-Vis spectra of **$[L_1H_3]$**, **$[L_1(BF_2)_3]$,** and **$[L_1(BPh_2)_3]$** compounds are studied at range 2.10^{-5}-2.10^{-7} mol L^{-1} in DMF

Figure 4. The emission spectra of fluorine triboron **$[L_{1\text{-}4}(BF_2)_3]$** complexes are studied at range 2.10^{-5}-2.10^{-7} mol L^{-1} in $CHCl_3$

Figure 5. The emission spectra of phenyl triboron **$[L_{1\text{-}4}(BPh_2)_3]$** complexes are studied at range 2.10^{-5}-2.10^{-7} mol L^{-1} in $CHCl_3$

Figure 6. The effect of the hemi-salen **(L_3H_3)** ligand on cell growth of human prostate cancer PC-3 cells

Figure 7. After treatment with the hemi-salen **(L_3H_3)** ligand different concentration (2.5-25 μM), or vehicle in **PC-3** cells, intracellular reactive oxygen species levels were assessed by flow fluometry

Figure 8. Effect of compound L_3H_3 on apoptosis of human prostad cancer **PC-3** cells

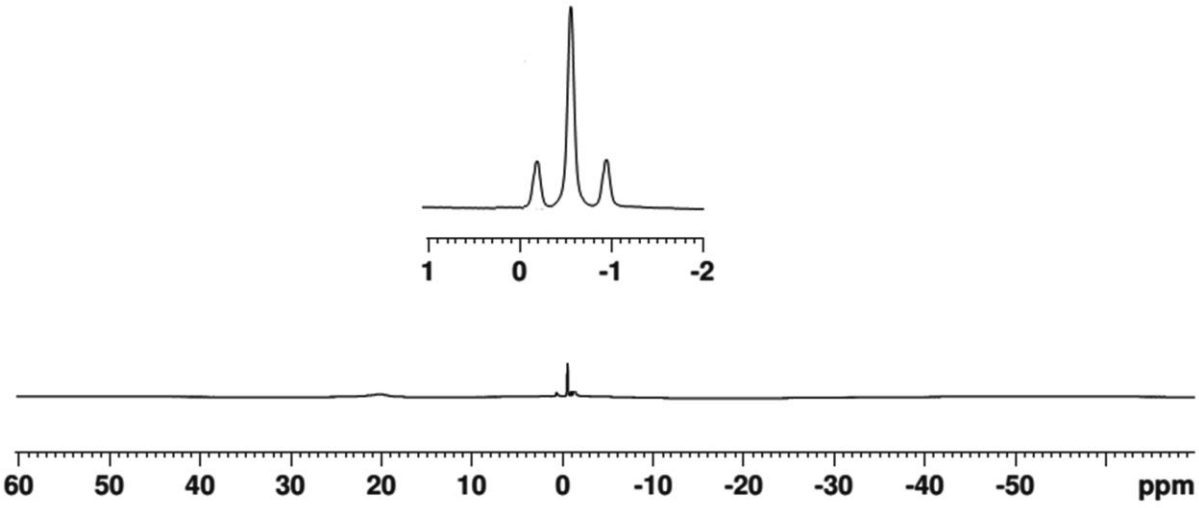

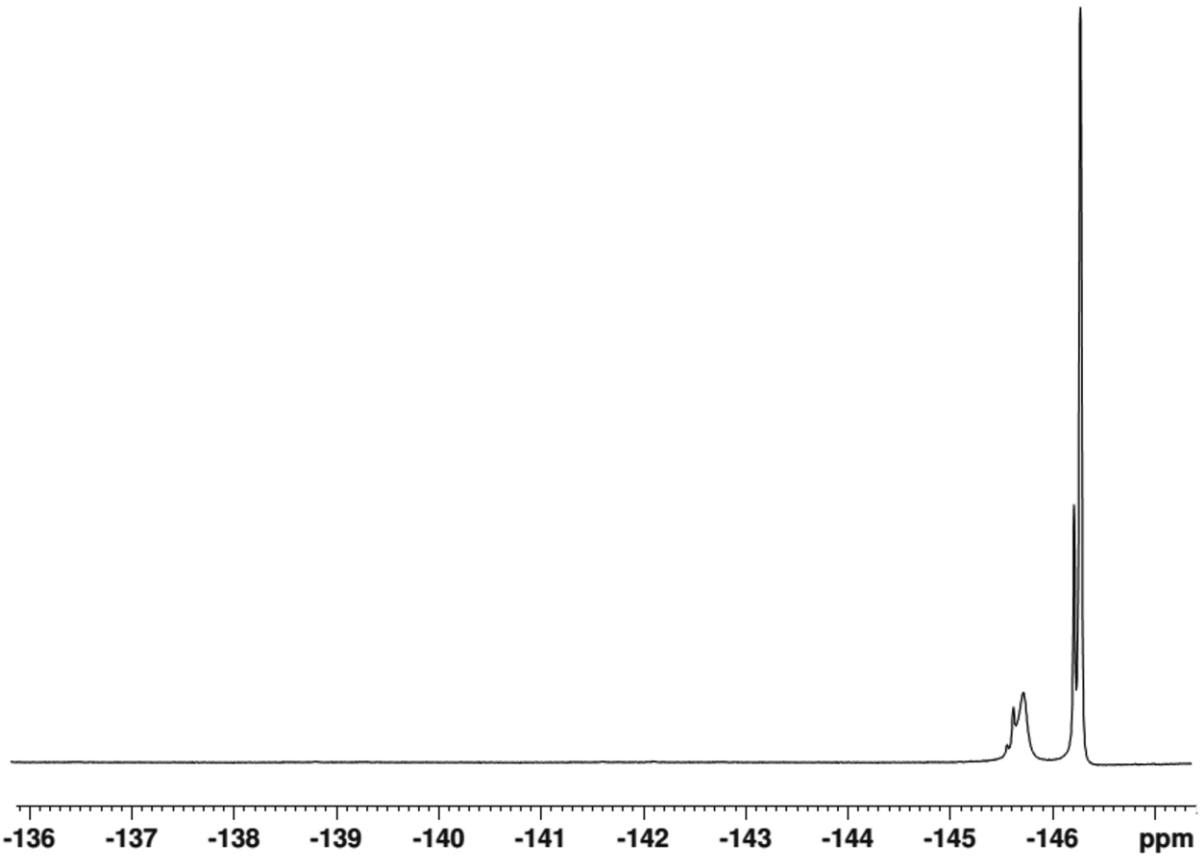

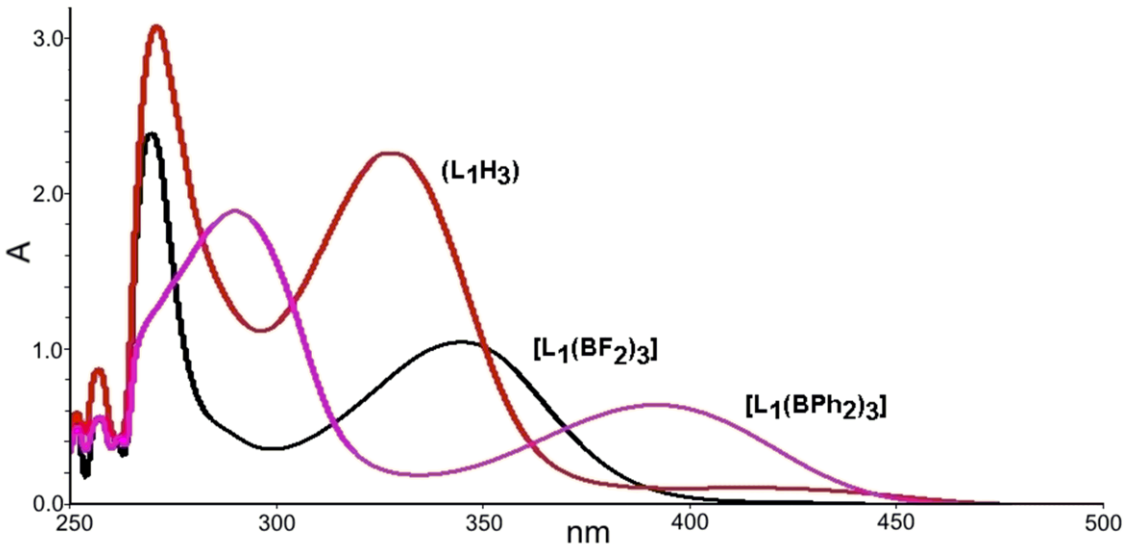

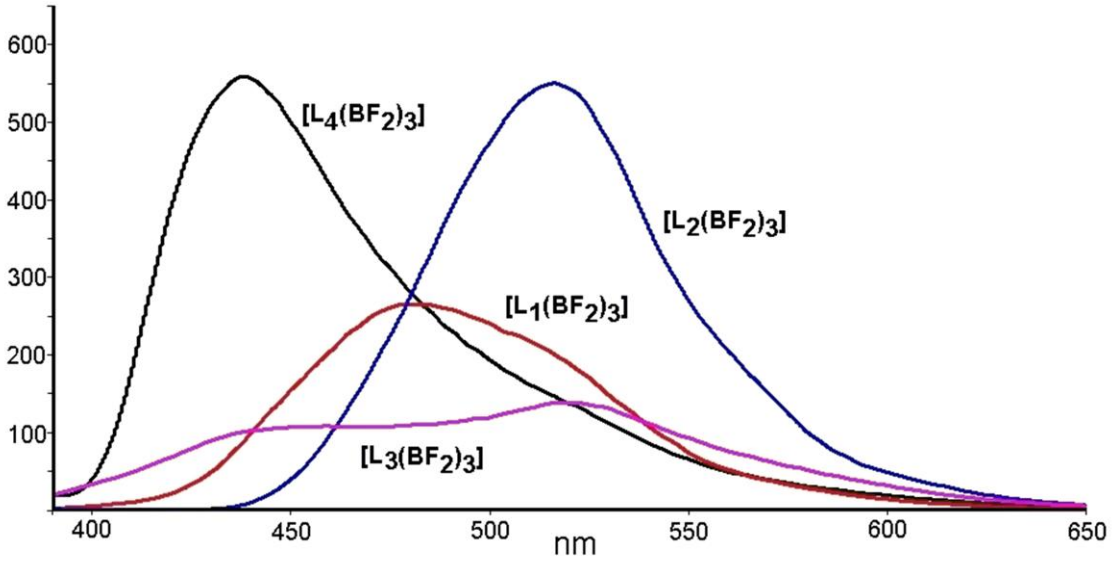

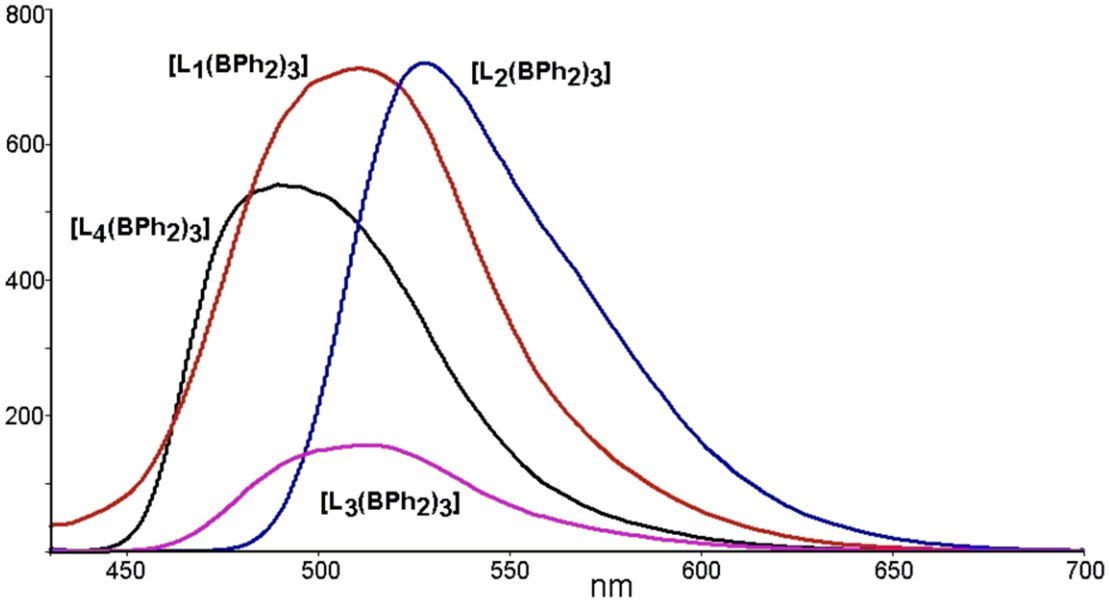

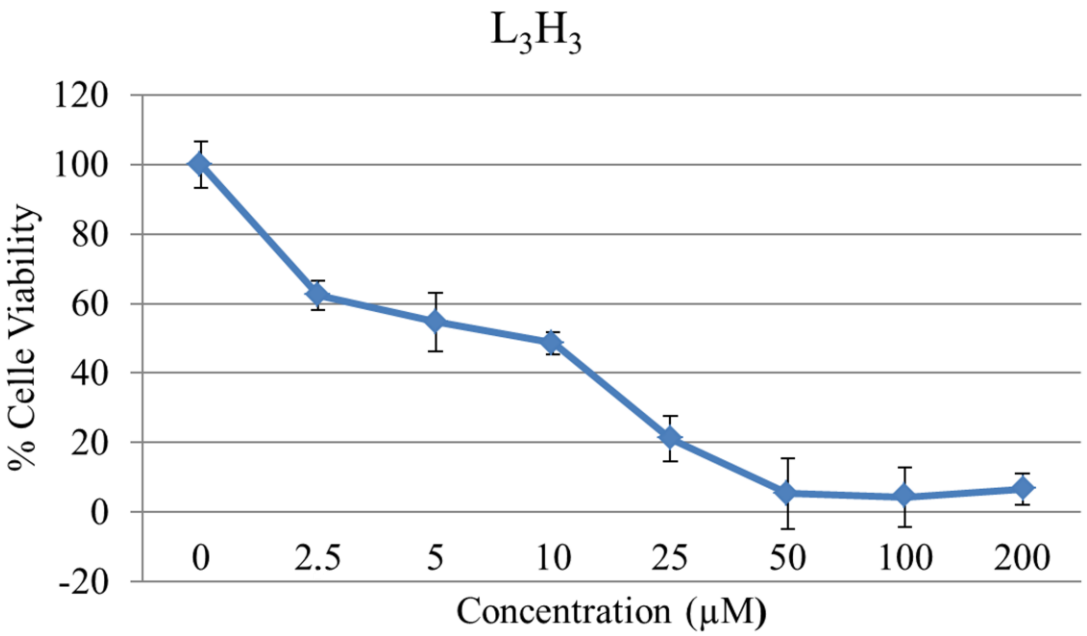

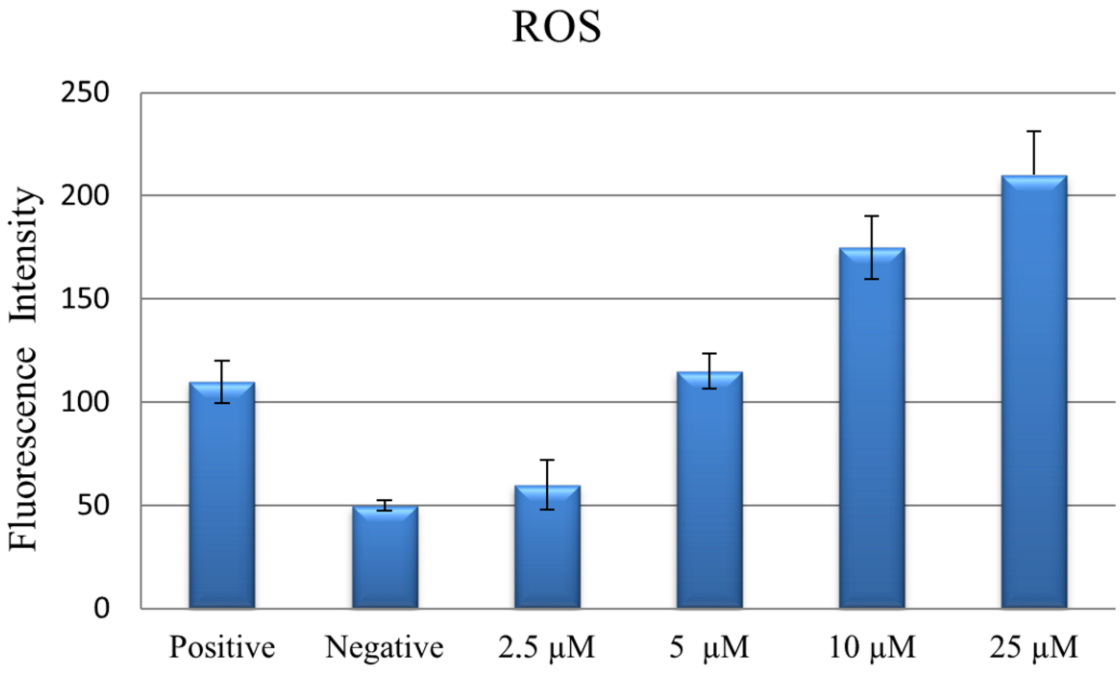

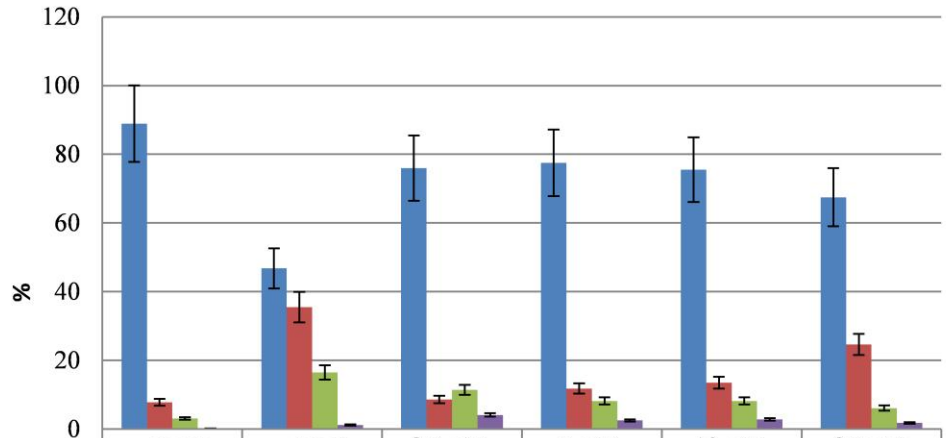

	neg(-)	poz(+)	2.5 µM	5 µM	10 µM	25 µM
Live	88.9	46.8	76	77.5	75.5	67.5
Early Apoptotic	7.8	35.5	8.6	11.8	13.5	24.6
Late Apoptotic	3.1	16.5	11.4	8.2	8.2	6.1
Necrotic	0.2	1.2	4.1	2.5	2.8	1.8

Negative

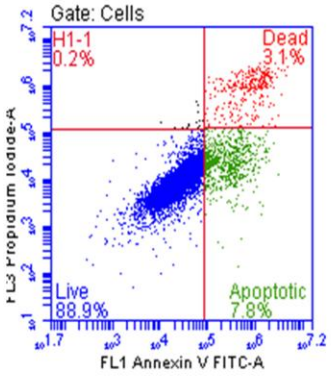

Positive

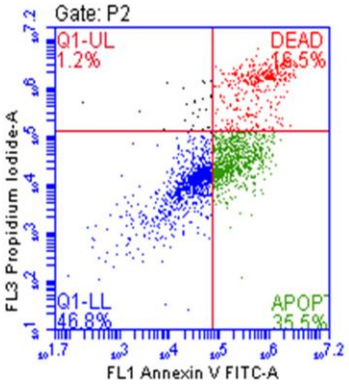

2.5 µM

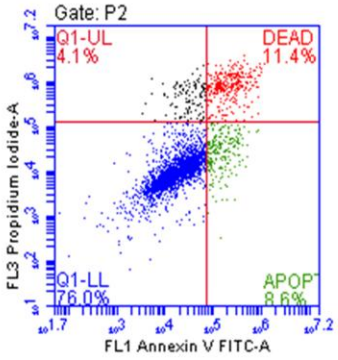

5 µM

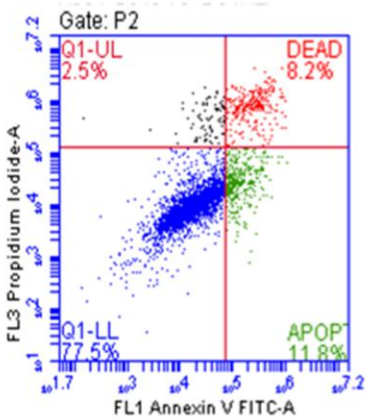

10 µM

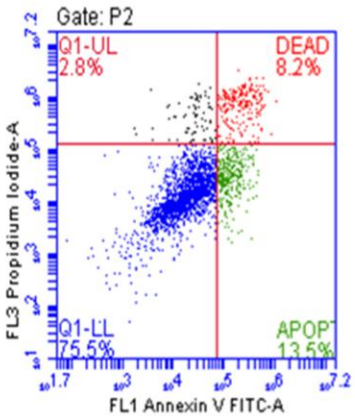

25 µM